Leading edge erosion and particle-laden turbulent flow: effects of the turbulence intensity and presence of gravity

S. Reza Hassanian. M
The Faculty of Industrial Eng. Mechanical Eng. and Computer Sci., University of Iceland
Reykjavik 102, Iceland
Email: *seh@hi.is*

ABSTRACT

This study presents results from a laboratory 3D turbulent flow experiment simulating a stagnation point at the leading edge of a wind turbine to investigate erosion caused by airborne particles. In a separate experiment, the flow is seeded with tracer and inertial particles, and the Taylor microscale Reynolds number (Re_λ) ranges from 100 to 150 and undergoes vertical strain deformation with a mean rate of 8 s^{-1}. The Lagrangian particle tracking (LPT) technique is employed to measure particle motion in the presence of gravity—a factor that has not been thoroughly examined in numerical studies due to its complexity and computational cost. Each experiment, conducted at varying turbulence intensities, is repeated 20 times to ensure statistically robust measurements. The influence of turbulence intensity is analyzed, and results show that increasing turbulence intensity leads to a 19%–23% increase in the erosion ratio. The normalized Reynolds stress indicates that inertial particles experience greater fluctuations than tracers under the same turbulence intensity. Moreover, higher turbulence intensity has a more pronounced effect on tracer particles. Since inertial particles are heavier than tracers, they could be more strongly influenced by gravity.

Keywords: *Wind turbine, energy, leading edge, erosion, turbulence.*

1. *INTRODUCTION*

Wind energy is the fastest-growing energy source in the world and is gaining increasing attention [1,2]. It is a clean, sustainable resource that can be generated both onshore and offshore. Recent innovations in clean energy production, particularly the combination of wind and solar power plants, have significantly enhanced wind power utilization [3]. Furthermore, with advances in hydrogen energy harvested from water, the demand for electricity from green and clean sources has made wind and solar energy increasingly attractive options [3,4].

One key advantage of wind power is its higher efficiency compared to other renewable resources [5]. For example, many meteorological stations, geological sites, and telecommunications towers are located in off-grid areas and primarily rely on diesel generators for electricity. While solar energy is a potential alternative, photovoltaic (PV) panels face several limitations due to weather and geographical conditions [5,6]. In many regions, sunlight hours are short in winter; cloudy weather reduces energy production; rain and snow can cover panels and halt production; and PV systems often require land rental or purchase for installation. In areas affected by sandstorms, PV panels can be covered with dust and sand, requiring costly automated cleaning systems or manual maintenance to ensure consistent energy generation [7].

In contrast, wind power overcomes many of these challenges and offers greater flexibility [5,6]. Wind turbines can operate effectively in windy, rainy, or snowy conditions. Unlike solar energy, cloud cover and darkness do not impact wind energy production [7]. Wind turbines also require only a single tower for installation, reducing land use [5]. Additionally, in contrast to horizontal-axis wind turbines (HAWTs), the advancements in vertical-axis wind turbines (VAWTs) have further improved the adaptability and efficiency of wind energy systems [5,6].

Leading-edge erosion of wind turbines is a significant issue, known to reduce their efficiency [8,9]. The current study focuses on horizontal-axis wind turbines (HAWTs) and investigates how airborne particles *contribute to erosion under various turbulence intensities in wind flow. Wind velocity exhibits turbulent behavior [3]; however, turbulence is still not fully understood [10], particularly in the presence of suspended particles [9,11]. The interaction between these particles and the turbulent structures adds further complexity to the problem [11]. Additionally, the effects of coherent flow structures remain unclear [1,12]. Recent studies on particle-laden turbulent flows have emphasized that observations from numerical simulations conducted without considering gravity cannot be directly applied to scenarios where gravity is present [13]. Therefore, it is essential to examine the influence of gravity on particles suspended in turbulent flow in real-world conditions.*

This study investigates the behavior of particles that contribute to leading-edge erosion, using a 3D experimental simulation of turbulent flow seeded with tracer and inertial particles. The flow undergoes strained deformation with various turbulence intensities to examine their effects on particle dynamics. It is well known that strain deformation can simulate a stagnation point [9,14], which is representative of conditions at the leading edge of a wind turbine blade. The erosion ratio is measured under different scenarios. Furthermore, the normalized Reynolds stress [10] of the particles is evaluated to examine the effects of turbulence intensity and the resulting fluctuations on erosion.

The study employs Particle Image Velocimetry (PIV) [15] to extract flow characteristics and Lagrangian Particle Tracking (LPT) [10] to analyze particle motion. Although LPT is also known as Particle Tracking Velocimetry (PTV) [16,17], the term LPT is used here to emphasize the Lagrangian framework of the approach. The paper is organized as follows: Section 2 outlines the theoretical background; Section 3 describes the experimental setup, particle tracking techniques, and statistical data extraction methods; Section 4 presents the results and discussion; and Section 5 provides the conclusions.

2. *Theory*

This section describes the theory of the turbulent flow and Lagrangian framework and how it can be used to study turbulent flow in statistical approaches [10,18]. In turbulent flow research, the statistical properties of flow characteristics are widely recognized and utilized [19]. The Lagrangian approach offers a powerful perspective for studying fluid motion by tracking the velocity and displacement vectors of individual points within the flow, referred to as fluid particles [19,20]. These fluid particles move in accordance with the local velocity of the surrounding fluid, thereby allowing their position to be identified at any given time, t [16]. Mathematically, a fluid particle is defined as follows [19]:

$$x_i=x_i\left(t,x_{i,0}\right), \qquad i=1,2,3 \qquad (1)$$

$$U_i=U_i\left(t,x_1\left(t,x_{1,0}\right),x_2\left(t,x_{2,0}\right),x_3\left(t,x_{3,0}\right)\right) \qquad (2)$$

equations (1) and (2) define the fluid particle's position and velocity in 3D coordinates, respectively, where x denotes position, U velocity, t time, and subscript i indicates the vector component. In the current study, the turbulence intensity has been created with the action of impeller rotors in the corners of a box turbulence facility. The turbulent flow has been strained in the vertical direction (see Figure 1) by the motion of flat circular plates, as shown in the sketch. Equation (3) defines the mean velocity field of the flow [10]:

$$\langle U\rangle=(Sx,-2Sy,Sz) \qquad (3)$$

where –2S is the primary strain rate in the Y-dir, and S is the mean strain rate for the other two directions, x, y and z are the particle location. In this work, the flow is measured in 2D, therefore, the Z-direction is not addressed. Note that the experimental data preserve the inherent three-dimensionality of turbulence [21]. The straining flow case in the experiment is generated with a mean strain rate of $2S = 8\ s^{-1}$. Although equation (3) is derived for laminar flow, it is important to note that velocity fluctuations occur in turbulent flow. The Stokes number for a seeded particle is calculated to verify whether the tracer particle behaves appropriately—specifically, whether it follows the flow streamlines. This behavior is characterized by equation (4):

$$St=\frac{\tau_p}{\tau_\eta} \quad (4)$$

where τ_p is Stokes' relaxation time. Kolmogorov scale (τ_η , defined in equation (6)) is based on the flow quantities before applying the strain. Stokes' relaxation time τ_p is in turn calculated by equation (5):

$$\tau_p=\frac{\rho_p d_p^{\ 2}}{18\mu} \quad (5)$$

where ρ_p is particle density, d_p is a spherical particle diameter and μ is the dynamic fluid viscosity that, in the conducted experiment, is water.

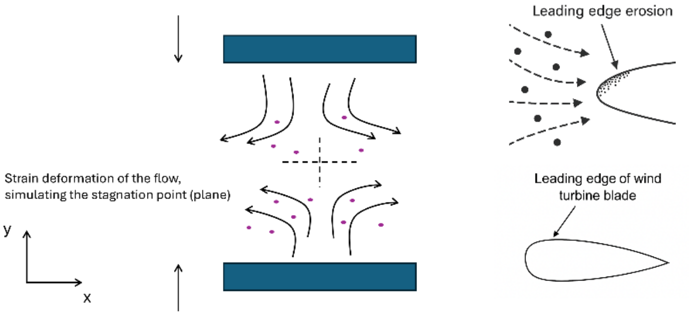

Fig. 1. *Schematic representation of the simulation showing the stagnation plane (or point) and the location of the leading edge.*

The Stokes number significantly greater than 1 ($St\gg 1$) describes particles that are unaffected by a fluid velocity change and continue their original trajectory; if $St\ll 1$, the particle will follow the fluid's local velocity. To extract the flow properties, the particle image velocimetry method (PIV) has been employed and once dissipation rate specified via second-order longitudinal velocity structure-function, Kolmogorov scales calculated by:

$$\tau_\eta=\left(\frac{v}{\varepsilon}\right)^{1/2} \quad (6)$$

where v is kinematic viscosity of the fluid, τ_η is the Kolmogorov's time scale and ε is dissipation rate evaluated via second-order longitudinal velocity structure-function. The Stokes number for the tracer particles used in the performed experiment are in the range of 0.0063–0.0094.

3. *Experiment setup*

The experiment is conducted at the Laboratory of Fundamental Turbulence Research (LFTR) at Reykjavik University, using the facility shown in Figure 2. The water tank, measuring 60 cm × 60 cm × 60 cm, is constructed with 20 mm-thick transparent acrylic walls (Plexiglas XT), allowing full optical access for data acquisition. The eight corners of the tank are triangular in shape, while the top and bottom surfaces are nearly circular. An aluminum frame secures the components of the turbulence box.

Turbulence is generated by eight impellers, each driven by an independently controlled servo motor (Lenz model: MCS), mounted at the eight corners and directed toward the center of the tank. The rotation speed of each motor can be adjusted between 100 and 4500 rpm, with a gear ratio of 0.075. The motion-view filtering software provided with the motors was utilized to configure and monitor the impeller speeds.

Before the experiment, a degassing system is employed to remove air bubbles and solid particles from the water. The tank is specifically designed for turbulence studies, enabling the investigation of both Lagrangian and Eulerian dynamics at moderate Reynolds numbers. The flow facility generates nearly stationary, homogeneous, and isotropic turbulence at the tank's center, where the measurements are carried out.

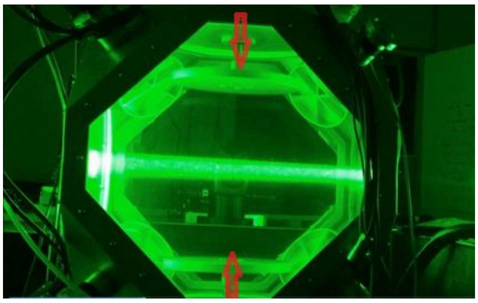

Fig. 2. *A photograph of the experiment captured at the moment of strain deformation.*

Circular plates positioned at the top and bottom of the tank (see Figure 1) generate the straining motion. Each plate is driven by a linear actuator with a piston rod (Parker, model: ETV32M10PA47JMA400A). When the plates move toward the center at a predetermined rate, they induce a nearly constant strain rate in the fluid.

The flow is seeded with spherical, hollow glass beads with a median diameter of 8–10 µm and a specific gravity of 1.1 g/cm³ for tracer particles. In contrast, the inertial particles are solid glass spheres with a median diameter of 220–250 µm and a specific gravity of 2.1 g/cm³. The recording region, located at the center of the tank, covers an area of 24.5 × 24.5 mm² (see Figure 1). Particle Tracking Velocimetry (PTV) is employed to capture flow properties prior to the onset of strain deformation. Using a second-order longitudinal velocity structure function, the turbulence dissipation rate is determined. This allows for the calculation of the Kolmogorov time scale (based on equation 6) and the Stokes number (from equation 4).

In this study, the strain rate produced by the two circular plates is 8 s^{-1}. Lagrangian particle tracking techniques are applied to analyze the data. A high-speed camera, operating at 10 kHz (10,000 frames per second), is used as the detection system, providing high temporal resolution (0.1–0.2 ms), which is significantly smaller than the Kolmogorov time scale (τ_η = 35–99 ms) of the smallest eddies in the flow. As a result, the dissipation-range properties are well-resolved.

Each video consists of 2,000 frames. To ensure sufficient statistical sampling, the straining motion was repeated 20 times, producing 20 independent videos and a total of 40,000 frames. Each video is statistically independent, as the flow is allowed ample time to return to near-isotropic conditions between successive straining events.

4. *Erosion ratio at stagnation point (assumed plane)*

The flow near the stagnation point in the experiment closely resembles that found near objects with natural stagnation points, such as the leading edge of a turbine blade, a compressor blade, or a rotor vane. The investigation of particle collisions with the stagnation plane is based on the following principles and methods: (a) Lagrangian Particle Tracking (LPT): This method allows the trajectory of each individual particle to be tracked from the moment it enters the observation region until it exits, (b)Two-particle state near the stagnation plane: As particles move around the streamlined body, two distinct behaviors are observed—some particles cross the stagnation plane, while others continue along their path without crossing it.

Based on the measured data, the total number of particles in each experiment is used to calculate the erosion ratio (ER), defined as the number of particles crossing the stagnation plane divided by the total number of particles. An increase in this ratio indicates a higher likelihood of erosion, while a decrease suggests reduced erosion.

5. *Results and discussion*

This section presents the results and discusses how turbulence intensity influences leading-edge erosion caused by airborne particles, as simulated in the experiment. The erosion ratio (ER) is determined by measuring the number of particles crossing the assumed stagnation plane under different turbulence intensities.

Table 1 displays the measurements of the erosion ratio. Since the experiment was performed with a constant strain rate, the effect of increasing turbulence intensity—from Re_λ = 100 to 150—can be directly *observed. For tracer particles, the ER increased from 26% to 49%. For inertial particles, the ER rose from 28% to 47% under the same conditions.*

These results indicate a direct correlation between turbulence intensity and erosion ratio, suggesting that higher turbulence intensities lead to increased erosion by suspended particles in the flow.

Table 1. Erosion ratio is measured based on the particles that are tracked and crossed the stagnation plane.

Turbulence intensity	*Strain rate (2S)*	*Particle type*	*Erosion ratio*
Re_λ=100	*8*	*Tracer*	*26%*
Re_λ=100	*8*	*Inertial*	*28%*
Re_λ=150	*8*	*Tracer*	*49%*
Re_λ=150	*8*	*Inertial*	*47%*

Moreover, the normalized Reynolds stress is analyzed to examine how turbulence intensity affects particle motion. Normalization is based on the Reynolds stress of the turbulent flow prior to the application of strain deformation. When strain deformation is introduced, it imposes an additional effect on the initially homogeneous and nearly isotropic flow, which is seeded only with tracer particles.

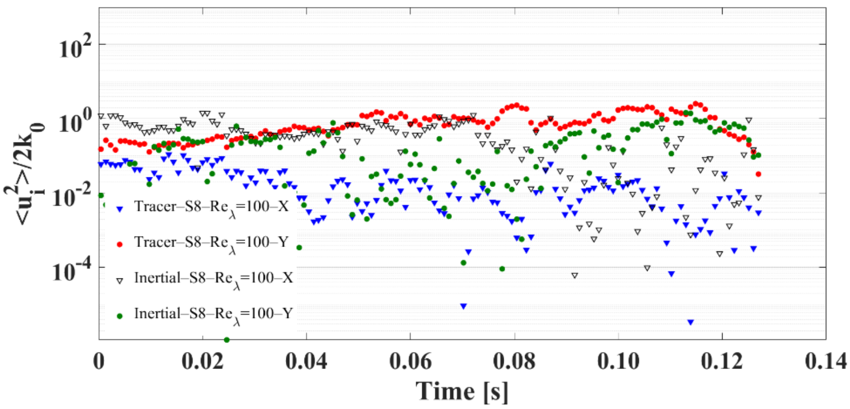

Fig. 3. *A photograph of the experiment captured at the moment of strain deformation*

Figures 3 and 4 illustrate the normalized Reynolds stress for tracer and inertial particles. Since the strain deformation occurs along the Y-direction, increased fluctuation is observed in that direction. As Reλ increases from 100 to 150, the normalized Reynolds stress also increases for both tracer and inertial particles.

The normalized Reynolds stress indicates that inertial particles experience greater fluctuations than tracers under the same turbulence intensity. However, the distribution pattern of the scattered points for inertial particles remains relatively unchanged. This may be attributed to their inertial behavior, which is influenced by gravity. It suggests that the dynamics of inertial particles are correlated not only with turbulence intensity but also with gravitational effects.

Turbulent flow is highly sensitive to perturbations and initial conditions. Large-scale structures can also play a significant role in influencing particle dynamics. As shown in Figures 3 and 4, the response to strain deformation exhibits a noticeable delay—particles begin to display the effects only after a short time lag. This delayed response may be attributed to the energy transfer from large to small scales within the turbulent flow.

Furthermore, the initial response of inertial particles differs from that of tracer particles. Inertial particles, influenced by their mass and response time, react differently to the deformation, highlighting the distinct dynamics between the two particle types.

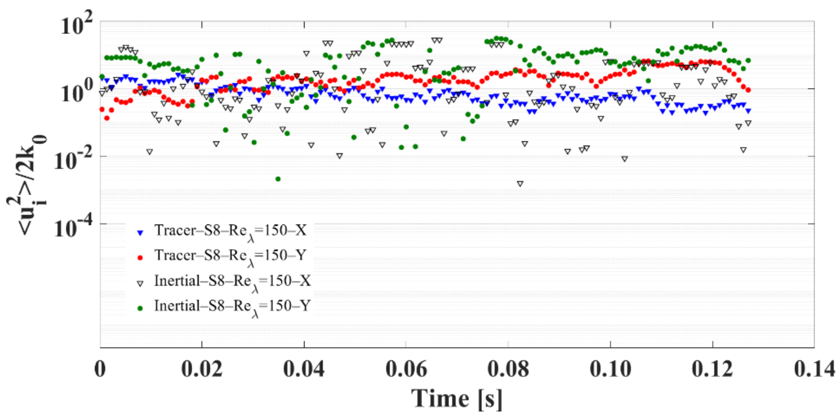

Fig. 4. *A photograph of the experiment captured at the moment of strain deformation*

6. *Conclusions*

This study presents an experimental investigation of turbulent flow subjected to strain deformation, simulating a stagnation plane (or point), to examine leading-edge erosion on a wind turbine rotor. The flow is seeded separately with tracer and inertial particles. Prior to the application of strain, the flow characteristics—including dissipation rate, strain rate, Reynolds number, Kolmogorov scale, and particle Stokes number—are measured using Particle Image Velocimetry (PIV).

Following the introduction of strain deformation, Lagrangian Particle Tracking (LPT) is employed to analyze particle motion. To evaluate erosion at the assumed stagnation plane, two scenarios are considered: (a) particles that cross the stagnation plane, indicating potential erosion, and (b) particles that do not cross, indicating no erosion. The flow is simulated at two turbulence intensity levels, corresponding to Reynolds numbers $Re_\lambda = 100$ and $Re_\lambda = 150$.

The results indicate a direct correlation between turbulence intensity and the erosion caused by airborne particles. It seems that inertial particles, due to their greater mass, also show sensitivity to gravitational effects. Additionally, a time lag in particle response to strain deformation is observed, suggesting that large-scale turbulence and energy transfer to smaller scales influence particle behavior.

This study provides insight into the inertial subrange of turbulent flow and particle dynamics, which contributes to the understanding of particle-laden turbulence and erosion mechanisms on wind turbine blades. These findings can support the development of protective coatings and erosion mitigation strategies. Moreover, the dataset from this experiment could be valuable for machine learning and deep learning applications in predicting turbulent flow behavior and leading-edge erosion, including potential clustering analyses.

REFERENCES

[1] *I. E. A. (IEA). (2021) Global energy review 2021 [Online] Available: https://www.iea.org/reports/global-energy-review-2021*

[2] *G. W. E. Council. (2021) Global wind report 2021 [Online] Available: https://gwec.net/wp-content/uploads/2021/03/GWEC-Global-Wind-Report2021.pdf*

[3] *Hassanian, R., Shahinfar, A., Helgadóttir, Á., & Riedel, M. (2024). Optimizing Wind Energy Production: Leveraging Deep Learning Models Informed with On-Site Data and Assessing Scalability through HPC. Acta Polytechnica Hungarica, 21(9), 45-56.*

[4] *N. R. Deevela, T. C. Kandpal, and B. Singh, "A review of renewable energy based power supply options for telecom towers," Environment, Development and Sustainability, Vol. 2023.*

[5] *Hassanian, R., Myneni, H., Helgadóttir, Á. and Riedel, M "Vertical Axis Wind Turbine Powers Telecom Towers: Green and Clean Configuration," 2023 6th International Conference on Electrical Engineering and Green Energy (CEEGE), Grimstad, Norway, 2023, pp. 114-118.*

[6] *Hassanian, R., Helgadóttir, Á. and Riedel, M., "A wake loss model asymmetry induced by the circulation of a vertical axis wind turbine," 2023 International Conference on Future Energy Solutions (FES), Vaasa, Finland, 2023, pp. 1-5.*

[7] *Hassanian, R.; Yeganeh, N.; Riedel, M. Wind Velocity and Forced Heat Transfer Model for Photovoltaic Module. Fluids 2024, 9, 17.*

[8] *Schramm, M.; Rahimi, H.; Stoevesandt, B.; Tangager, K. The Influence of Eroded Blades on Wind Turbine Performance Using Numerical Simulations. Energies 2017, 10, 1420*

[9] *Hassanian, R.; Riedel, M. Leading-Edge Erosion and Floating Particles: Stagnation Point Simulation in Particle-Laden Turbulent Flow via Lagrangian Particle Tracking. Machines 2023, 11, 566.*

[10] *Hassanian, R., Helgadóttir, Á., Bouhlali, L., Riedel, M.,; An experiment generates a specified mean strained rate turbulent flow: Dynamics of particles. Physics of Fluids 1 January 2023; 35 (1): 015124.*

[11] *Hassanian, R., Helgadóttir, Á., Gharibi, F., Beck, A., Riedel, M.; Data-driven deep learning models in particle-laden turbulent flow. Physics of Fluids 1 February 2025; 37 (2): 023348.*

[12] *Hassanian, R., Myneni, H., Helgadóttir, Á. and Riedel, M; Deciphering the dynamics of distorted turbulent flows: Lagrangian particle tracking and chaos prediction through transformer-based deep learning models. Physics of Fluids 1 July 2023; 35 (7): 075118.*

[13] *Brandt, L. and Coletti, F., " Particle-laden turbulence: Progress and perspectives," Annu. Rev. Fluid Mech. 54, 159–189 (2022)*

[14] *C.-M. Lee, Á. Gylfason, P. Perlekar, and F. Toschi, " Inertial particle acceleration in strained turbulence," J. Fluid Mech. 785, 31–53 (2015).*

[15] *M. R. J. Kompenhans, C. E. Willert, F. Scarano, C. J. Kähler, and S. T. Wereley, Particle Image Velocimetry (Springer International Publishing, 2018).*

[16] *E. A. Cowen, S. G. Monismith, E. A. Cowen, and S. G. Monismith, "A hybrid digital particle tracking velocimetry technique," Exp. Fluids 22, 199–211 (1997).*

[17] *N. T. Ouellette, H. Xu, and E. Bodenschatz, "A quantitative study of three-dimensional Lagrangian particle tracking algorithms," Exp. Fluids 40, 301–313 (2006).*

[18] *Hassanian, R.; Helgadóttir, Á.; Riedel, M. Deep Learning Forecasts a Strained Turbulent Flow Velocity Field in Temporal Lagrangian Framework: Comparison of LSTM and GRU. Fluids 2022, 7, 344.*

[19] *S. B. Pope, Turbulent Flows (Cambridge University Press, 2000).*

[20] *Hassanian, R.; Aach, M.; Lintermann, A.; Helgadóttir, Á.; Riedel, M. Turbulent Flow Prediction-Simulation: Strained Flow with Initial Isotropic Condition Using a GRU Model Trained by an Experimental Lagrangian Framework, with Emphasis on Hyperparameter Optimization. Fluids 2024, 9, 84.*

[21] *H. T. John and L. Lumley, A First Course in Turbulence (MIT Press, 1972).*